TENTH AUSTRALASIAN FLUID MECHANICS
CONFERENCE - UNIVERSITY OF MELBOURNE
11-15 DECEMBER 1989

QUANTITATIVE MAPPING OF PARTICLE DISPERSION IN AN AXIALLY FORCED ROUND JET

Ellen K. LONGMIRE and John K. EATON

Mechanical Engineering Department
Stanford University
Stanford, CA 94305
USA

ABSTRACT

A two-phase flow consisting of 55 micron diameter solid particles in an axisymmetric air jet was investigated experimentally. An acoustic speaker forced the flow at single or double frequencies to organize the vortex ring structures forming downstream of the jet nozzle exit. Phase-specific photographs of a vertical slice of forced flow at $Re_D = 19000$ were processed to examine the distribution of the particles. The results corroborate earlier flow visualization studies in which relatively more particles were found in the highly strained saddle regions between the vortex rings. Also, for flow forced at a Strouhal number based on jet diameter of 0.5 or lower, few or no particles were located inside the rings.

INTRODUCTION

Many experiments have been performed on particle-laden jet flows including the recent work of Mostafa *et al.* (1989), Fleckhaus *et al.* (1987), and Shuen *et al.* (1985). These experiments have yielded measurements of mean and fluctuating velocities of both the gas and solid phases. The above results provide detailed information about the time-averaged behavior of such jets, but yield little insight into the instantaneous interaction of particles and turbulent structures.

In practical applications where solid or liquid particles must be injected into combustion chambers, process streams, or reaction vessels, the instantaneous rather than time-averaged distribution of the particles is often important. In a combusting or reacting flow, the reaction kinetics are largely determined by the local conditions surrounding an individual particle. For example, particles concentrated in a dense group might experience radically different reaction conditions from a particle located far from any others.

Numerous studies have shown the importance of vortex ring structures in the near field of turbulent jets. Significant control has been exhibited by relatively simple forcing schemes designed to organize the vortex motions. The present study attempts to extend the understanding of single-phase jets to gas jets laden with fine solid particles. In particular, we wish to determine the effects of the vortex ring structures on the instantaneous particle concentration field.

Experimental results in two-dimensional mixing layers (Lazaro and Lasheras (1989), Kamalu *et al.* (1988), and Masutani *et al.* (1987)) suggest that for particles of appropriate time scale, large-scale vortical structures do affect particle dispersion. Numerical computations involving two-dimensional vortex pairing (Chein and Chung (1987)) and an axisymmetric jet (Chung and Troutt (1988)) have also demonstrated that large-scale flow structures can influence particle motion. Finally, recent analytical and numerical studies of homogeneous turbulence (Maxey (1987), Hunt *et al.* (1988), and Squires and Eaton (1989)) have shown that particles of appropriate time scale may actually be concentrated in convergence zones of the turbulence. In light of the above results, the present study attempts to examine the effects of vortex rings of different length scales on particle dispersion (or concentration) and also to control local particle dispersion by manipulating the vortex ring structures.

EXPERIMENTAL PROCEDURE

Jet Facility

Two facilities were used to generate the data for the present study. Originally, particles and air were injected into a 4 inch diameter plenum and accelerated through a 25-to-1 area ratio nozzle with an exit diameter of 2 cm. Flow visualization and other previously reported studies (see Longmire and Eaton (1989)) were completed in this facility. A second nozzle-plenum combination was constructed with a plenum diameter of 2 inches. The nozzle has a 6.45-to-1 area contraction ratio to reach the same exit diameter of 2 cm. The smaller contraction ratio of the new nozzle alleviates the problem of particles flying toward the jet axis downstream of the nozzle exit as well as problems of particles accumulating on the nozzle surface.

The experimental set-up is depicted in Figure 1. Pressurized air supplied by a compressor passes to the jet plenum through either a bypass line or a fluidized bed of glass particles. Particles which elutriate from the top of the fluidized bed are also fed to the jet plenum. By varying the bed height and the relative amounts of air flowing through either of the two lines, the mass loading ratio of particles to air can be varied from zero to 1.0. Air and particles reaching the jet plenum pass through a honeycomb grid before entering the nozzle. For the flow visualization studies, the jet nozzle was directed vertically upward, but the orientation was changed to eliminate particle accumulation within the jet plenum. The change in orientation had little effect on the flow structure.

The particles are glass beads sized to 50-60 micron diameter with a Vortec air classifier. Average particle density was measured as 2.4 g/cc. These properties yield a particle time scale based on Stokes drag of 22 ms.

Qualification studies on the single-phase unforced jet with a hot wire showed a top-hat shaped profile at the nozzle exit with turbulence levels in the core region on the order of 1%. Measurements of tangential velocity with a laser Doppler anemometer indicated no significant swirl.

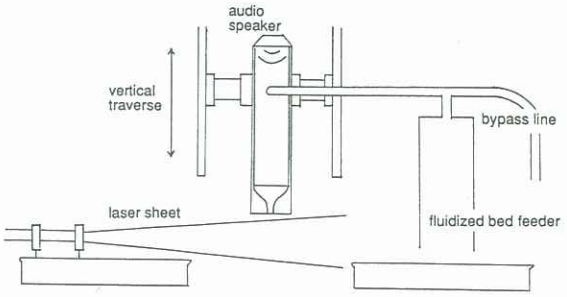

Figure 1. Particle-laden jet facility.

An ordinary audio speaker located on top of the plenum forces the flow at specific frequencies to organize the vortex ring structures which normally roll up in the free shear layer downstream of the nozzle exit. An IBM XT computer generates and outputs the desired forcing waveforms which are routed through a low-pass filter and amplifier before reaching the speaker.

A pulsed copper vapor laser beam formed a vertical sheet for flow visualization studies. The laser pulsing frequency was controlled by the computer and coupled with the jet speaker forcing to create either a strobing effect for flow visualization or a single phase-locked pulse. Both videotape and 35mm film were used to capture the strobed and instantaneous flow. For other details on the experimental facility, see Longmire and Eaton (1989).

Processing Technique

For the quantitative number density studies presented below, the jet was operated at a low mass loading (5-11%) providing a relatively low number density. Single pulse photographs were then obtained at known forcing phase. To provide reference points for data analysis, three illuminated pinholes were located the same distance from the camera as the laser sheet and imaged onto the focal plane with a mirror. All photographs were printed on 8"x10" sheets so that individual particles could be identified easily.

Printed photographs were scanned to produce binary image matrices using a DEST Scanner interfaced with a Macintosh II computer. Software first decoded the image matrix into the corresponding full bit map representation. A second routine searched the bit map file to identify all contiguous objects and computed each object's centroid, pixel area, and moment of inertia. These values were then used as criteria for identifying particles and fiducial marks. The area (number of pixels in an object) could vary for a single particle from 1 up to about 50 depending on the particle's position within the laser sheet, because scattering from particles in the center of the sheet was much more intense than that from particles near the sheet's edges. A moment of inertia criterion was used to differentiate round objects from elongated ones. The two criteria described above were employed not only to identify individual particles, but also to identify overlapping ones. Once the fiducial marks and particles were located, the entire system was translated into real-scale coordinates.

Files of particle positions were converted into two-dimensional maps of number density. A rectangular grid of points spaced at 2 mm intervals served as the basis for the map. The number density at each of the four grid points surrounding each particle was incremented according to the exact particle position. (*e.g.* If the particle was equidistant from the four nearest grid points, the number density associated with each point was incremented by 1/4.) Each map was normalized by the total number of particles counted. Photographs covered the range between x/D of 0 and 8, and typically contained about 1700 particles. In order to produce smooth mappings, the results from 25 photographs were summed and normalized for each case and phase of flow studied.

Results are illustrated with a gray scale screen plotter where each block in an image corresponds to one of the grid points. The scale runs from white, equaling maximum normalized number density, down to dark gray. In a typical plot, a "white" grid point represents about 170 particles counted, while a "dark gray" grid point represents a minimum of 10 particles counted. Each increment in the scale represents about 15 additional particles counted.

RESULTS AND DISCUSSION

Single Frequency Forcing

Particle-laden flow at Re_D = 19000 was subject to axial forcing with a single frequency. The flow was forced at Strouhal numbers of 0.5 and 0.9 with the input forcing amplitude to the speaker generating the velocity fluctuation levels listed in Table 1. The mass loading ratio of glass beads to air was 8% for StD = 0.5 and 5% for StD = 0.9.

Table 1. Jet Forcing Amplitudes

frequency(Hz)	St_D	u'/U
360	0.5	0.110
648	0.9	0.045
360+180(0)	0.5+0.25	0.110
360+180(90)	0.5+0.25	0.086

The structure of smoke-marked single-phase flow is shown in Figure 2. Although the flow conditions do not exactly match those for the particle-laden flow, the scales of the structures seen are very similar. The lower frequency forcing generates large, regularly spaced vortex rings which persist beyond x/D = 6 (the limit of the laser sheet). The higher frequency forcing yields smaller, more tightly spaced vortices which also remain coherent until x/D of at least 6.

A typical single pulse photograph from the St_D = 0.5 particle-laden case is depicted in Figure 3. Note the regularly spaced bunches of particles occurring along the jet axis between the vortex ring locations. Particles move away from the jet axis by passing through the highly strained saddle regions. The particles gain radial momentum from the fluid on the downstream edge of each vortex ring and are propelled outward. Also, the regions containing the vortex rings are devoid of particles.

The number density maps for the two frequencies investigated are presented in Figure 4. For St_D = 0.5, two phases of flow are shown. The images indicate that the clusters of particles begin forming at x/D = 0.5 and maintain approximately the same shape until x/D = 6.5. The local number density in the clusters gradually decreases with increasing axial distance as particles are continuously convected outward in the saddle regions.

The number density map of the St_D = 0.9 case appears entirely different. This forcing frequency was chosen as the upper limit at which the vortex ring structures could be seen to affect the particle paths. Some evidence of weak particle clustering can be seen between x/D of 1 and 3. In general, however, the number density of particles decreases monotonically with increasing axial distance and also with increasing radial distance. The map is exactly what one

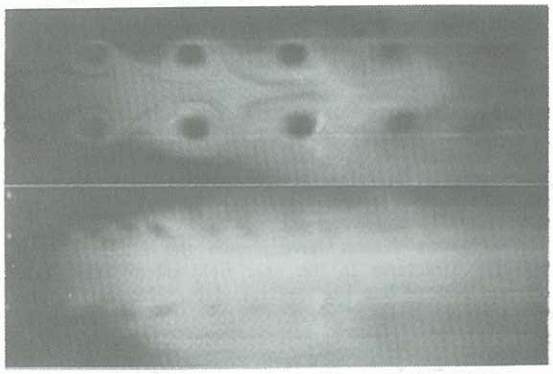

Figure 2. Smoke visualization; Re_D = 23000; Upper: St_D = 0.42; Lower: St_D = 0.93.

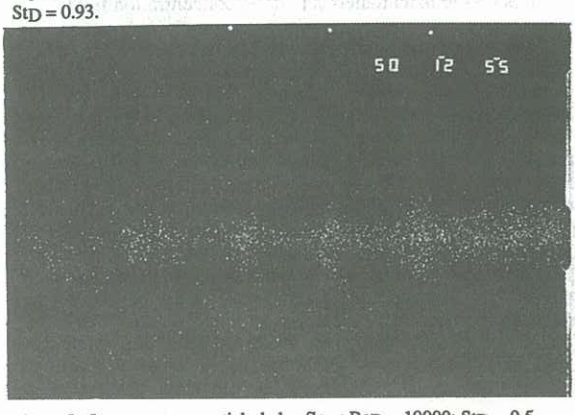

Figure 3. Instantaneous particle-laden flow; Re_D = 19000; St_D = 0.5.

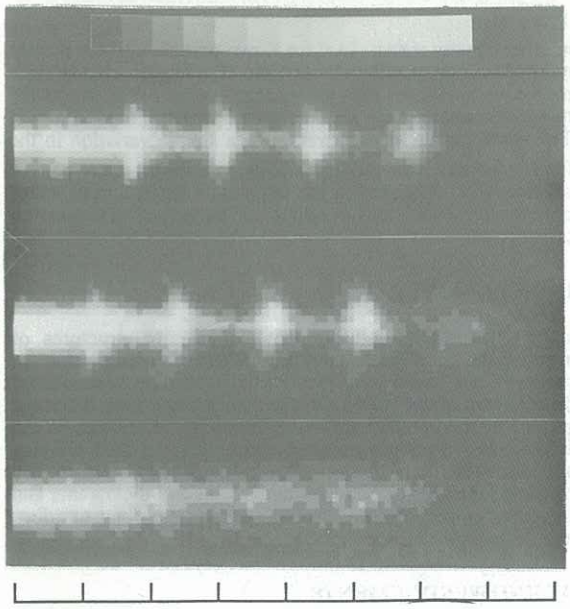

Figure 4. Composite number density maps; Re_D = 19000; Upper: St_D = 0.5; Lower: St_D = 0.9;

would expect to see in a diffusion-type model of particle dispersion.

Subharmonic Forcing

When the flow is forced with two waves, a fundamental plus a subharmonic, a pairing of the vortex rings occurs. By varying the relative phases of the summed waves, the nature and axial location of the pairing can be altered significantly. For the number density studies, flow was forced with two equal amplitude sine waves at St_D = 0.5 and St_D = 0.25. Two cases were studied: phase = 0 (I) and phase = 90 (II). The resultant waveforms are plotted in Figure 5, and the nozzle exit velocity fluctuation levels are listed in Table 1. Particle-to-air mass loading ratio varied from 6 to 11 percent. Flow conditions were otherwise identical to those in the single frequency cases.

Visualizations of the single-phase flow for Cases I and II are found in Figures 6 and 7. Again, the conditions do not exactly match those of the particle-laden flow, but the qualitative behavior is very similar. In Figure 6 (phase = 0), the vortex pairing occurs at x/D of about 4.3 whereas in Figure 7 (phase = 90) the pairing occurs at x/D = 3. The pairing process also differs significantly in the two cases. In Case I, the upstream vortex in each pair completely loses its identity at pairing. In Case II, however, the upstream vortex of the pair passes through its counterpart completely and is convected outward before it apparently breaks down.

Number density maps of four different phases of the

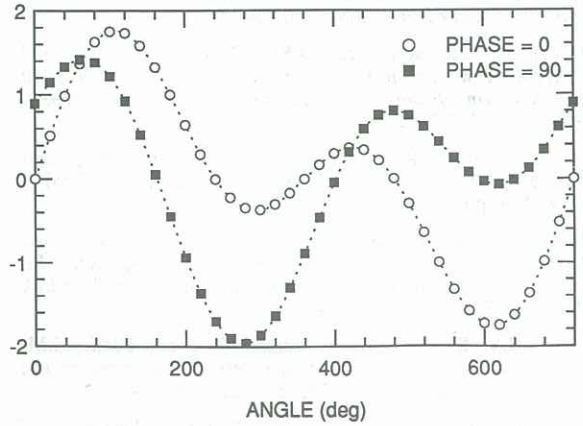

Figure 5. Fundamental + Subharmonic.

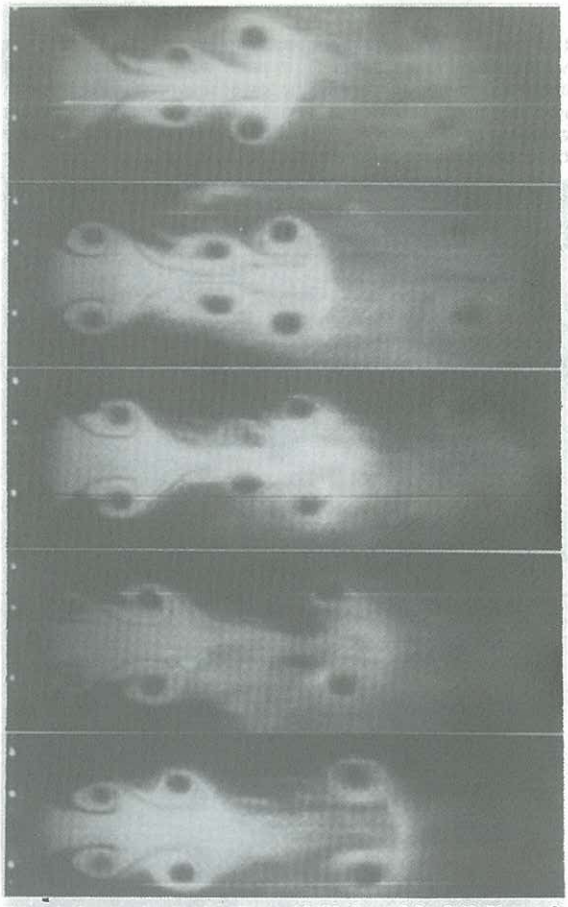

Figure 6. Smoke visualization; Re_D = 23000; St_D = 0.21+0.42; Phase = 0.

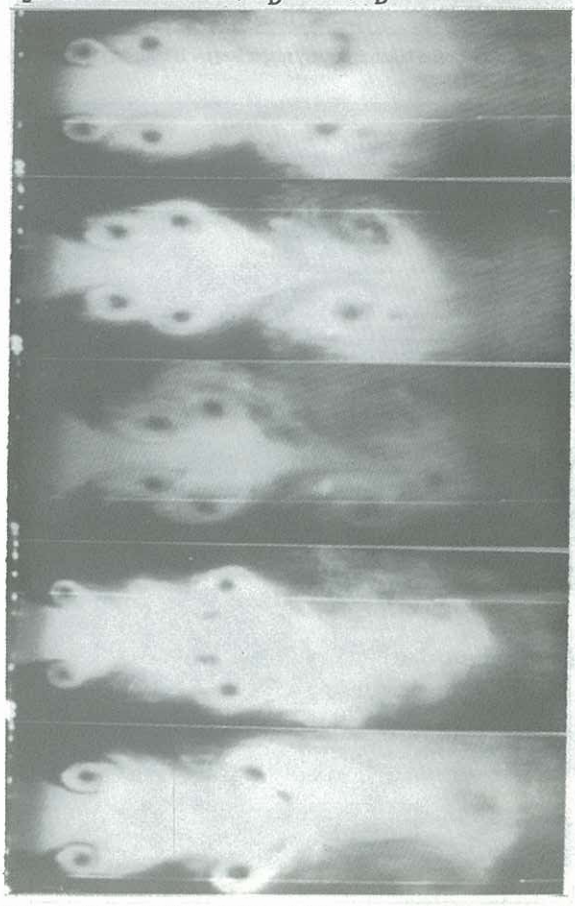

Figure 7. Smoke visualization; Re_D = 23000; St_D = 0.21+0.42; Phase = 90.

two cases are depicted in Figures 8 and 9. In Case I, the lower vortex ring breaks down as it pairs with the upper ring at about x/D = 4.5. In Case II, the lower ring propagates through its counterpart at x/D = 3, and both rings apparently remain coherent until x/D > 6. The differing flow structures in the two cases produce different particle distribution patterns in the

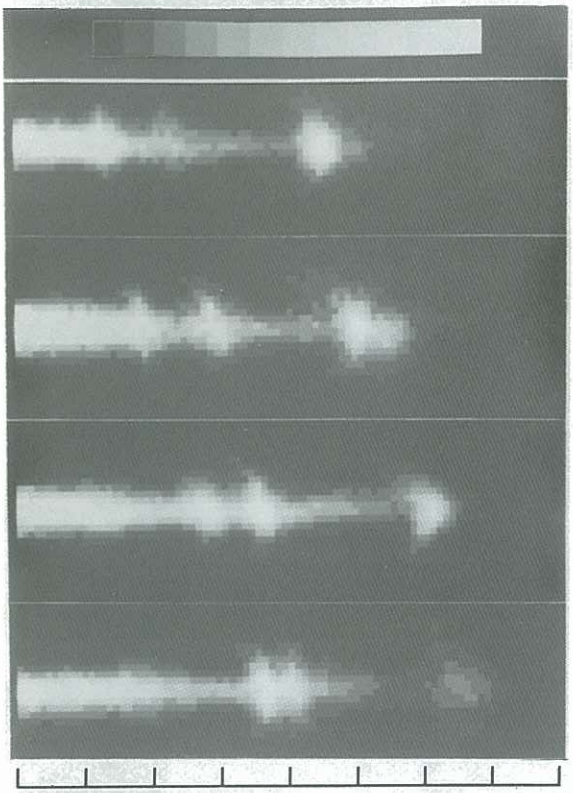

Figure 8. Composite number density maps; Re_D = 19000; St_D = 0.25+0.5; Phase = 0.

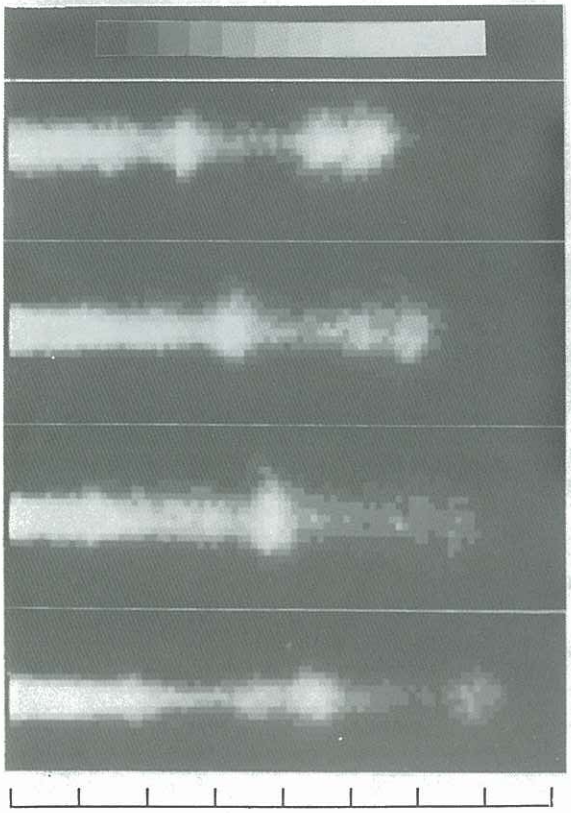

Figure 9. Composite number density maps; Re_D = 19000; St_D = 0.25+0.5; Phase = 90.

number density maps. In Case I, two particle clusters clearly merge into one at x/D = 5. In Case II, however, two clusters merge as one vortex ring passes through the other, but as the two rings separate, the single cluster is redistributed into two. The above results demonstrate how a simple variation in the forcing pattern can modify the particle distribution pattern substantially. Changes in the large-scale jet structures cause changes in the locations of strong concentrations or dispersion of particles.

CONCLUSIONS

The results indicate that vortex ring structures of appropriate time scale strongly affect the dispersion of particles in a round jet flow. Particles become concentrated downstream of the vortex rings and are thrown away from the jet axis by the outwardly moving fluid in these regions. When large-scale vortex rings are present, this outward flinging appears to be the primary particle dispersion mechanism. By manipulating the vortex ring length scales and the manner and locations of pairing, the positions of particle concentrations and dispersion can be controlled.

ACKNOWLEDGEMENTS

This work was funded by the Electric Power Research Institute under Contract No. RP 8005-2. The first author was supported by fellowships from the Link Foundation and the American Association of University Women.

REFERENCES

Chein, R. and Chung, J.N. (1987) "Effects of Vortex Pairing on Particle Dispersion in Turbulent Shear Flows", *International Journal of Multiphase Flow*, **13**, pp. 785-802.

Chung, J.N. and Troutt, T.R. (1988) "Simulation of Particle Dispersion in an Axisymmetric Jet", *Journal of Fluid Mechanics*, **186**, pp.199-222.

Fleckhaus, D., Hishida, K. and Maeda, M. (1987) "Effect of Laden Solid Particles on the Turbulent Flow Structure of a Round Free Jet", *Experiments in Fluids*, 5, pp. 323-333.

Hunt, J.C.R., Wray, A.A., and Moin, P. (1988) "Eddies, Streams, and Convergence Zones in Turbulent Flows", Center for Turbulence Research, *Proceedings of the Summer Program*, Stanford, CA.

Kamalu, N., Wen, F., Hanle, R., Chung, J.N., and Troutt, T.R. (1987) "Visualization of Particle Dispersion in Free Shear Flows", *Bulletin of the American Physical Society*, **32**, no. 10, page 2066.

Kobayashi, H., Masutani, S.M., Azuhata, S., Arashi, N., and Hishinuma, Y. (1987) "Dispersed Phase Transport in a Plane Mixing Layer", Second Int'l Symposium on Transport Phenomena in Turbulent Flows, Tokyo, pp. 693-706.

Lazaro, B.J. and Lasheras, J.C. (1989) "Particle Dispersion in Turbulent, Free Shear Flows", *Seventh Symposium on Turbulent Shear Flows*, Stanford, CA.

Longmire, E.K. and Eaton, J.K. (1989) "Structure and Control of a Particle-Laden Round Jet", *U.S.-Korea Joint Seminar on Fluids Engineering and Science*, Seoul, September, 1989.

Maxey, M.R. (1987) "The gravitational settling of aerosol particles in homogeneous turbulence and random flow fields", *JFM*, **174**, pp. 441-465.

Mostafa, A.A., Mongia, H.C., McDonell, V.G., and Samuelsen, G.S. (1989) "Evolution of Particle-Laden Jet Flows: A Theoretical and Experimental Study", *AIAA Journal*, **27**, no. 2, pp. 167-183.

Shuen, J.S., Solomon, A.S.P., Zhang, Q.F., and Faeth, G.M. (1985) "Structure of Particle-Laden Jets: Measurements and Predictions", *AIAA Journal*, **23**, no. 3, pp. 396-404.

Squires, K.D., and Eaton, J.K. (1989) "Study of the Effects of Particle Loading on Homogeneous Turbulence Using Direct Numerical Simulation", 3rd Joint ASCE/ASME Mechanics Conference, San Diego.